

Journal of Fluid Mechanics

<http://journals.cambridge.org/FLM>

Additional services for *Journal of Fluid Mechanics*:

Email alerts: [Click here](#)

Subscriptions: [Click here](#)

Commercial reprints: [Click here](#)

Terms of use : [Click here](#)



Attenuation of short surface waves by the sea floor via nonlinear sub-harmonic interaction

Mohammad-Reza Alam, Yuming Liu and Dick K. P. Yue

Journal of Fluid Mechanics / Volume 689 / December 2011, pp 529 - 540

DOI: 10.1017/jfm.2011.448, Published online: 08 November 2011

Link to this article: http://journals.cambridge.org/abstract_S0022112011004484

How to cite this article:

Mohammad-Reza Alam, Yuming Liu and Dick K. P. Yue (2011). Attenuation of short surface waves by the sea floor via nonlinear sub-harmonic interaction. Journal of Fluid Mechanics, 689, pp 529-540 doi:10.1017/jfm.2011.448

Request Permissions : [Click here](#)

Attenuation of short surface waves by the sea floor via nonlinear sub-harmonic interaction

Mohammad-Reza Alam^{1,2}, Yuming Liu¹ and Dick K. P. Yue^{1†}

¹ Department of Mechanical Engineering, Center for Ocean Engineering, Massachusetts Institute of Technology, Cambridge, MA 02139, USA

² Department of Mechanical Engineering, University of California, Berkeley, CA, 94720, USA

(Received 29 July 2011; revised 22 September 2011; accepted 9 October 2011;
first published online 8 November 2011)

We consider the indirect mechanism for dissipation of short surface waves through their near-resonant interactions with long sub-harmonic waves that are dissipated by the bottom. Using direct perturbation analysis and an energy argument, we obtain analytic predictions of the evolution of the amplitudes of two short primary waves and the long sub-harmonic wave which form a near-resonant triad, elucidating the energy transfer, from the short waves to the long wave, which may be significant over time. We obtain expressions for the rate of total energy loss of the system and show that this rate has an extremum corresponding to a specific value of the (bottom) damping coefficient (for a given pair of short wavelengths relative to water depth). These analytic results agree very well with direct numerical simulations developed for the general nonlinear wave–wave and wave–bottom interaction problem.

Key words: surface gravity waves, coastal engineering

1. Introduction

Recent observations report significant short-wave damping as they travel over dissipative (muddy) seafloors (see e.g. Sheremet & Stone 2003; Sheremet *et al.* 2005; Elgar & Raubenheimer 2008). An explanation via classical linearized theory (e.g. Dalrymple & Liu 1978; Macpherson 1980; Myrhaug 1995; Ng & Zhang 2007) is not immediately available since the short wave apparently does not interact with the bottom. Nonlinear effects have been believed to play a role although the precise mechanism remains uncertain in part due to the absence of rigorous theory and quantitative predictions.

This work is motivated by recent suggestion (e.g. Sheremet *et al.* 2005) that the dissipation of short waves might result from their nonlinear coupling with long waves which are directly affected by bottom dissipation. In numerical simulations of nonlinear conoidal wave propagation over viscous muds, Kaihatu, Sheremet & Holland (2007) observed that the amplitude of high-frequency wave components could be reduced by the dissipation of sub-harmonic wave components, supporting the hypothesis of Sheremet *et al.* (2005). Matching field observations with simulations from a nonlinear Boussinesq wave model, Elgar & Raubenheimer (2008) obtained the dissipation rate of the mud bottom as a function of wave frequency and water depth

† Email address for correspondence: yue@mit.edu

showing that the dissipation of long (infragravity) waves dominates that of short waves. The detailed mechanism for these, however, has not been fully elucidated.

Alternative mechanisms have also been proposed. Recently, Mei *et al.* (2010) found through a perturbation analysis with a visco-elastic mud model that long waves can be dissipated through the slow modulation of short waves. This effect was also observed by Torres-Freyermuth & Hsu (2010) in simulations based on the Reynolds-averaged Navier–Stokes equations of two-layer fluids. The predictions, however, do not qualitatively explain the observations of Sheremet *et al.* (2005) and Elgar & Raubenheimer (2008).

To investigate the nonlinear mechanism suggested by Sheremet *et al.* (2005) and Elgar & Raubenheimer (2008) for the dissipation of short waves by their nonlinear interactions with long waves that are directly affected by bottom dissipation, we consider a canonical problem involving the nonlinear evolution of two short surface waves and their corresponding sub-harmonic long wave. Such a three-wave system does not satisfy exact resonance conditions for water waves except in the limit of (non-dispersive) shallow water (Mei & Unluata 1971; Young 1998). For water depth shallow relative to the long (sub-harmonic) wave, however, the requisite dispersion relationship is almost satisfied. Under this almost resonant condition, the triad undergoes nonlinear evolution that involves energy exchange among the three components. Our interest is in this nonlinear evolution in the case where the sub-harmonic wave is subject to direct (bottom) damping. Of special interest is the rate at which the energy in the short waves, and generally that of the overall system, is dissipated.

We perform a perturbation analysis coupled with an energy argument to derive the governing equations for the three-wave system, and obtain analytic solutions, to leading order, for the nonlinear evolutions of respectively the sub-harmonic long wave and the short primary waves. The results provide quantitative predictions for the (short-wave) dissipation mechanism in support of earlier conjecture. For the general practical problem that may involve multiple such (near-resonant) interactions, we apply a direct numerical simulation based on the high-order spectral method (Dommermuth & Yue 1987; Liu & Yue 1998). The perturbation theory predictions are confirmed well by the direct numerical results.

2. Governing equations

We consider the irrotational motion of a homogeneous inviscid incompressible fluid with a free surface. The water depth, h , is assumed to be constant, surface tension is ignored, and surface slopes, ϵ , are small such that perturbation theory applies. Consider a Cartesian coordinate system with its origin located on the calm water surface with positive z oriented upward. In terms of the velocity potential ϕ , the fully nonlinear governing equations in two dimensions are

$$\nabla^2 \phi = 0, \quad (2.1a)$$

$$\phi_{tt} + g\phi_z + \beta\phi_t + \partial_t(\phi_x^2 + \phi_z^2) + \frac{1}{2}(\phi_x\partial_x + \phi_z\partial_z)(\phi_x^2 + \phi_z^2) = 0, \quad z = \eta, \quad (2.1b)$$

$$\phi_z = 0, \quad z = -h, \quad (2.1c)$$

in which β represents the (frequency dependent) damping due to bottom dissipation, g is the acceleration due to gravity, and the surface elevation is $\eta = -[\phi_t + (\phi_x^2 + \phi_z^2)/2]/g$ evaluated on $z = \eta$.

Consider two propagating free waves given by

$$\eta(x, t) = a_1 \sin(k_1x - \omega_1t) + a_2 \sin(k_2x - \omega_2t), \quad (2.2)$$

where k_i , ω_i , a_i , $i = 1, 2$, respectively represent the wavenumber, frequency and amplitude of each wave. For free propagating waves, k_i and ω_i satisfy the dispersion relation, $\omega_i^2 = gk_i \tanh k_i h$. We are interested in the characteristics and development of the sub-harmonic wave, wavenumber $k_- = k_1 - k_2$ and frequency $\omega_- = \omega_1 - \omega_2$, associated with the (second-order) interaction of these two free waves. For general finite depth, k_- , ω_- cannot also satisfy the dispersion relationship, hence the three waves cannot form a resonant triad (see e.g. Hasselmann 1962; Young 1998). The exception is in the non-dispersive shallow water limit, wherein such triads are associated with harmonic generation, resulting in transfer of energy among the harmonics (see e.g. Goda 1967; Mei & Unluata 1971; Bryant 1973; Alam & Mei 2007).

Our interest is the case where k_1 , k_2 are relatively close and the water depth is finite but small relative to the long sub-harmonic wave. In this case, the dispersion relationship is approximately satisfied:

$$(\sqrt{gk_- \tanh(k_- h)} - \omega_-) / \omega_- \equiv \mu \ll 1. \quad (2.3)$$

This near-resonance condition is a case of bound interaction, wherein the energy associated with the short k_1 , k_2 waves may be continuously transferred to the long k_- wave if the latter is damped, for example, through bottom interactions. This scenario is of practical importance especially when bottom conditions such as that of a muddy seafloor provide effective damping of the long wave. For example, significant damping of short waves in muddy regions has been reported by Sheremet & Stone (2003) and Sheremet *et al.* (2005).

The effect of bottom dissipation, expressed by β in (2.1b), decreases exponentially with decreasing wavelength (for relatively short waves) and is given, say, by $\beta \sim \exp(-\sigma kh)$, where σ is a (positive) constant (see for instance Dalrymple & Liu 1978; Macpherson 1980; Kaihatu *et al.* 2007). The ratio of the damping rates between the short primary and long sub-harmonic waves is thus scaled by: $\exp[-\sigma(k_i - k_-)h]$, $i = 1, 2$. For sufficiently large $(k_i - k_-)h$, the damping of the short waves in (2.1) can therefore be ignored relative to the long wave.

3. Second-order perturbation solution

We solve (2.1) to second order using a regular perturbation expansion, in terms of small wave steepness ϵ . Writing $\phi = \epsilon\phi^{(1)} + \epsilon^2\phi^{(2)} + \dots$, at the second order (2.1) gives

$$\nabla^2\phi^{(2)} = 0, \quad (3.1a)$$

$$\phi_{tt}^{(2)} + g\phi_z^{(2)} + \beta\phi_t^{(2)} = -2\phi_x^{(1)}\phi_{xt}^{(1)} - 2\phi_z^{(1)}\phi_{zt}^{(1)} - \eta^{(1)}(\phi_{ttz}^{(1)} + g\phi_{zz}^{(1)}), \quad z = 0, \quad (3.1b)$$

$$\phi_z^{(2)} = 0, \quad z = -h. \quad (3.1c)$$

The right-hand side of (3.1b) contains quadratic forcing terms, resulting from the interactions of the (first-order) short free waves. In general, the second-order solution is small compared to the first-order solution unless a near-resonance condition (2.3) obtains (see e.g. Mei 1985; Kirby 1986, for near-resonance behaviours in other water wave systems). Our objective here is the small ($\omega_i t = o(1/\epsilon)$), initial, time evolution of the second-order sub-harmonic long wave, $\phi_-^{(2)} \equiv \phi_-$. In this time scale, the short waves are not modified to leading order, and a_1 and a_2 can be assumed constant.

Focusing on ϕ_- , and upon substitution of the leading-order result (2.2) into the right-hand side of (3.1b), we have

$$\phi_{-tt} + g\phi_{-z} + \beta_- \phi_{-t} = I_0 a_1 a_2 \sin[k_- x - \omega_- t], \tag{3.2}$$

in which $\beta_- = \beta(\omega_-)$, and

$$I_0 = \frac{\omega_1 \omega_2}{4gk_1 k_2 \sinh k_1 h \sinh k_2 h} (C_1 \cosh k_- h + C_2 \sinh k_- h + C_3 \cosh k^+ h + C_4 \sinh k^+ h) \tag{3.3}$$

where $k^+ = k_1 + k_2$, $C_1 = \omega_1 g k_2^2 - \omega_2 g k_1^2$, $C_2 = \omega_2 k_1 \omega_1^2 + \omega_1 k_2 \omega_2^2$, $C_3 = C_1 - 4k_1 k_2 g \omega_-$, and $C_4 = \omega_2 k_1 \omega_1^2 - \omega_1 k_2 \omega_2^2$. The initial-value problem for ϕ_- can be solved using Fourier transform in x and Laplace transform in t . The solution (assuming zero initial condition) is finally given by

$$\begin{aligned} \phi_-(x, z, t) = & - \frac{I_0 a_1 a_2 \cosh k_-(z+h)}{2\alpha \left[(\omega_*^2 - \omega_-^2)^2 + \beta_-^2 \omega_-^2 \right] \cosh k_- h} \\ & \times \{ \mathcal{A} \cos[k_- x + \alpha t] + \mathcal{C} \cos[k_- x - \omega_- t] + \mathcal{E} \sin[k_- x + \alpha t] \\ & + \mathcal{B} \cos[k_- x - \alpha t] + \mathcal{D} \sin[k_- x - \omega_- t] + \mathcal{F} \sin[k_- x - \alpha t] \}, \end{aligned} \tag{3.4}$$

where $\omega_* = \sqrt{gk_- \tanh k_- h}$, $\alpha = \sqrt{4\omega_*^2 - \beta_-^2}/2$ and

$$\mathcal{A} = \beta_- \left(\alpha \omega_- - \frac{1}{2} \omega_-^2 - \frac{1}{2} \omega_*^2 \right) e^{-\beta_- t/2}, \quad \mathcal{C} = -2\alpha \beta_- \omega_-, \tag{3.5}$$

$$\mathcal{B} = \beta_- \left(\alpha \omega_- + \frac{1}{2} \omega_-^2 + \frac{1}{2} \omega_*^2 \right) e^{-\beta_- t/2}, \quad \mathcal{D} = 2\alpha (\omega_-^2 - \omega_*^2), \tag{3.6}$$

$$\mathcal{E} = (\alpha \omega_*^2 + \omega_-^3 - \omega_- \omega_*^2 + \frac{1}{2} \beta_-^2 \omega_- - \alpha \omega_-^2) e^{-\beta_- t/2}, \tag{3.7}$$

$$\mathcal{F} = (\alpha \omega_*^2 - \omega_-^3 + \omega_- \omega_*^2 - \frac{1}{2} \beta_-^2 \omega_- - \alpha \omega_-^2) e^{-\beta_- t/2}. \tag{3.8}$$

4. Near-resonance interaction without damping

If $\beta_- = 0$, (3.4) reduces to

$$\begin{aligned} \phi_-(x, z, t) = & - \frac{I_0 a_1 a_2 \cosh k_-(z+h)}{[\omega_-^2 - \omega_*^2] \cosh k_- h} \\ & \times \left\{ \sin[k_- x - \omega_- t] + \frac{\omega_-}{\omega_*} \cos k_- x \sin \omega_* t - \sin k_- x \cos \omega_* t \right\}. \end{aligned} \tag{4.1}$$

If we assume $\mu \ll 1$, the above equation can be further simplified to

$$\phi_-(x, z, t) = \frac{I_0 a_1 a_2 \cosh k_-(z+h)}{\mu \omega_-^2 \cosh k_- h} \sin \frac{\mu \omega_-}{2} t \cos[k_- x - \omega_- t]. \tag{4.2}$$

The surface elevation for ϕ_- is then given by

$$\eta_- = \int \phi_{-z}|_{z=0} dt = \frac{I_0 a_1 a_2 k_- \tanh k_- h}{\mu \omega_-^3} \sin \frac{\mu \omega_-}{2} t \sin[k_- x - \omega_- t]. \tag{4.3}$$

It is seen that the amplitude of the sub-harmonic wave is modulated by a period of $T_{mod} = 4\pi/(\mu\omega_-)$.

We note that (4.3) is obtained for the initial growth of ϕ_- valid for $\omega_i t = o(1/\epsilon)$, and derived under the assumption of constant a_1 and a_2 (to leading order). To obtain the solution for longer time ($\omega_i t = O(1/\epsilon)$), the time variation of a_1 and a_2 must now

be included. To do that, we apply an energy argument. In terms of the total potential ϕ and elevation η , in the absence of damping ($\beta = 0$), the total (average) energy of the wave system is conserved:

$$\bar{E} = \int dx \left\{ \frac{1}{2} \rho g \eta^2 + \int_{-h}^0 \frac{1}{2} \rho (\phi_x^2 + \phi_z^2) dz \right\} = \text{constant}. \tag{4.4}$$

For the present case of a three-wave system with (time evolving) amplitudes, i.e. short waves a_1 , a_2 and sub-harmonic long waves a_- , (4.4) has the form $\bar{E} = \sum_i q_i a_i^2$, where q_i are functions of $k_i h$ (only), and $i = 1, 2, -$. From the above, we obtain

$$\frac{d\bar{E}}{dt} = 2q_1 a_1 \frac{da_1}{dt} + 2q_2 a_2 \frac{da_2}{dt} + 2q_- a_- \frac{da_-}{dt} = 0. \tag{4.5}$$

Equation (4.5) can be satisfied by a solution of the form

$$\frac{da_1}{dt} = \gamma_1 a_2 a_- f(t), \quad \frac{da_2}{dt} = \gamma_2 a_1 a_- f(t), \quad \frac{da_-}{dt} = \gamma_- a_1 a_2 f(t), \tag{4.6}$$

where $f(t)$ is an arbitrary function of time, and $\gamma_1, \gamma_2, \gamma_-$ are constants satisfying $\sum_i q_i \gamma_i = 0$. Matching (4.6) for a_- to (4.3) valid for the initial growth of $a_-(t)$, we obtain

$$\gamma_- = \frac{I_0 k_- \tanh k_- h}{2\omega_-^2}, \quad f(t) = \cos(\mu\omega_- t/2). \tag{4.7}$$

Note that in the above solution of γ_- and $f(t)$, the slowly time-varying effect of $a_1(t)$ and $a_2(t)$ is not included as it gives a higher-order contribution to a_- within the time scale $\omega_i t = O(1/\epsilon)$. The solutions for the other amplitudes in the sub-harmonic triad, in terms of γ_1, γ_2 , can be obtained similarly starting with the regular perturbation solution for each. We note that a similar procedure can be used to obtain the solution to the problem of harmonic generation in shallow water, recovering, for instance, the results of Bryant (1973).

5. Near-resonance interaction with damping

We now consider a non-zero damping of the sub-harmonic long wave given by β_- . Equation (3.4) can be written in the form

$$\phi_-(x, z, t) = \frac{\omega_- I_0 a_1 a_2 \sqrt{\beta_-^2 + 4\mu^2 \omega_-^2} \cosh k_-(z+h)}{\left[(\omega_*^2 - \omega_-^2)^2 + \beta_-^2 \omega_-^2 \right] \cosh k_- h} \sin [k_- x + \omega_- t + \psi] + \text{TT}, \tag{5.1}$$

where $\psi = \arctan(\beta_-/2\mu\omega_-)$, and TT represents transient terms. The expression for TT is complicated but simplifies in the case of small damping $\beta_-/\omega_* \approx \beta_-/\omega_- \ll O(\mu)$. Under this assumption, we obtain from (3.4)

$$\begin{aligned} \phi_-(x, z, t) \approx & - \frac{2I_0 a_1 a_2 \mu \omega_*^3 \cosh k_-(z+h)}{\alpha \left[(\omega_*^2 - \omega_-^2)^2 + \beta_-^2 \omega_-^2 \right] \cosh k_- h} \\ & \times \left\{ \sin [k_- x - \omega_- t] - e^{-\beta_- t/2} \sin [k_- x - \alpha t] \right\}, \end{aligned} \tag{5.2}$$

which contains explicitly the two time-harmonic components: one with frequency ω_- and constant amplitude; and the other with frequency α and a time-decaying amplitude representing the initial transient effect.

The energy dissipation by the sub-harmonic wave can be calculated from the boundary-value problem (3.1). From (3.1b), the term containing β_- acts like an external pressure on the free surface, and the average rate of energy dissipation by this term can be calculated from

$$\frac{\overline{dE}}{dt} = \int dx Pw, \quad (5.3)$$

where $P = \rho\beta_-\phi_-$ is the equivalent pressure from the dissipation term, and $w = (\phi_-)_z$ is the vertical velocity of the free surface. Using (5.1), we obtain

$$\frac{\overline{dE}}{dt} \equiv \left(\frac{g}{h}\right)^{5/2} \frac{\rho}{g} a_1^2 a_2^2 \overline{F}, \quad \overline{F} = \left(\frac{h}{g}\right)^{5/2} \frac{\beta_- g I_0^2 \omega_-^2 k_- (\beta_-^2 + 4\mu^2 \omega_-^2) \tanh k_- h}{2 [(\omega_*^2 - \omega_-^2)^2 + \beta_-^2 \omega_-^2]}, \quad (5.4)$$

where the dimensionless average dissipation rate \overline{F} is independent of a_1 and a_2 .

Figure 1(a) shows a sample variation of \overline{F} as a function of ω_1 and ω_2 for a specific value of $\beta_- \sqrt{h/g}$. Clearly $\overline{F} = 0$ for $\omega_- = 0$, and \overline{F} generally increases with ω_- . Note that figure 1(a) is strictly valid only for $|\omega_1 - \omega_2|/(\omega_{1,2}) \ll O(1)$, an underlying assumption of the analysis so far. Figure 1(b) plots the variation of \overline{F} as a function β_-/ω_- for fixed $\omega_1 \sqrt{h/g}$ and $\omega_2 \sqrt{h/g}$. As expected, $\overline{F} = 0$ for $\beta_- = 0$. Interestingly, \overline{F} has an extremum at a particular value of $\beta_- = \beta_{-max}$. From (5.4), we can show that this extremum occurs at

$$\frac{\beta_{-max}}{\omega_-} = \frac{1}{2} \left[6\mathcal{A} - 24\mu^2 + 2(9\mathcal{A}^2 - 56\mu^2\mathcal{A} + 144\mu^2)^{1/2} \right]^{1/2}, \quad (5.5)$$

where $\mathcal{A} = [\omega_*^2 - \omega_-^2]^2 / \omega_-^4$. The maximum damping rate \overline{F}_{max} at β_{-max} is now obtained but the expression is complicated. Some simplification is obtained for the case of $\mu \ll 1$, yielding

$$\overline{F}_{max} \equiv \overline{F}|_{(\beta_- = \beta_{-max})} \approx \left(\frac{h}{g}\right)^{5/2} \frac{g I_0^2 k_- \tanh k_- h}{8\mu\omega_-^3}, \quad (5.6)$$

which shows explicitly the expected $\overline{F}_{max} \sim \mu^{-1}$ dependence.

Figures 2(a) and 2(b) respectively show the value of β_{-max} as a function of ω_1 and ω_2 ; and extremum energy dissipation rate \overline{F}_{max} . Note that β_{-max} generally increases for increasing $|\omega_-| = |\omega_1 - \omega_2|$. For given $|\omega_-|$, β_{-max} increases with $\omega_i \sqrt{h/g}$, as expected, so that a higher damping coefficient is required with greater frequency (relative to depth). In figure 2(b), for increasing $|\omega_1 - \omega_2|$, \overline{F}_{max} also increases, with a rate that is greater for small $\omega_i \sqrt{h/g}$. Note that each point in this figure corresponds to a different value of the damping coefficient β_{-max} , so that the contours of \overline{F}_{max} indicate the maximum damping rate achievable rather than its variation with $\omega_i \sqrt{h/g}$ for a given physical problem (cf. figure 1a).

We remark that the argument associated with (5.3) obtains the total damping rate of the system but not the (damped) evolution of a_1 , a_2 , which is one of the primary objectives of these analyses. To obtain these, we return to the form of the energy equation (4.6), but now include explicitly the effect of damping on a_- :

$$\frac{da_1}{dt} = \gamma_1 a_2 a_- f(t), \quad \frac{da_2}{dt} = \gamma_2 a_1 a_- f(t), \quad \frac{da_-}{dt} = \gamma_- a_1 a_2 f(t) - \nu_- a_-, \quad (5.7)$$

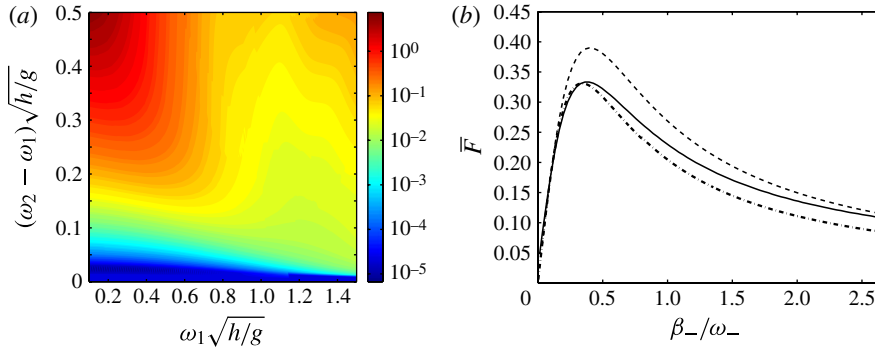


FIGURE 1. (a) Dimensionless damping rate \bar{F} (equation (5.4)) as a function of the frequencies of the primary short waves ω_1, ω_2 for damping coefficient $\beta_- \sqrt{h/g} = 0.11$. (b) Dimensionless damping rate \bar{F} as a function of damping coefficient β_- , for $\omega_1 \sqrt{h/g} = 0.48$ and $\omega_2 \sqrt{h/g} = 0.65$, obtained from: perturbation theory (5.4) (- - -); energy argument from (5.8) (- · -); and direct simulation (—).

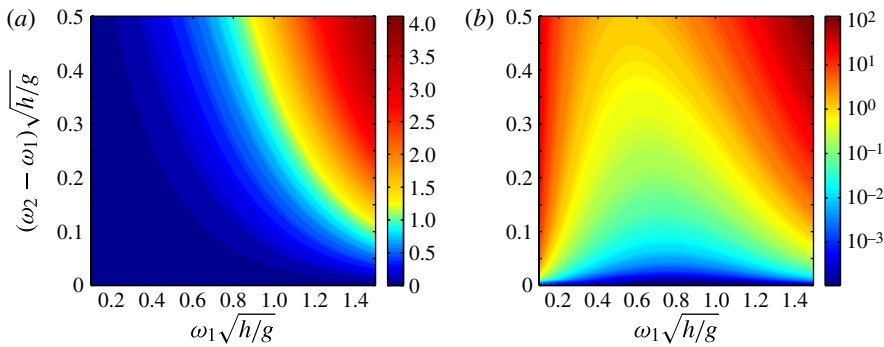


FIGURE 2. (a) Value of damping coefficient $\beta_{-max} \sqrt{h/g}$ (equation (5.5)) for maximum damping rate as a function of ω_1, ω_2 . (b) Maximum damping rate \bar{F}_{max} (equation (5.6)) as a function of ω_1, ω_2 .

where ν_- is the damping coefficient in this model. The evolutions $a_1(t), a_2(t)$ can be obtained by integration once ν_- is known, and the solution is complete if ν_- can be related to the original damping coefficient β_- .

To achieve that, we match the total dissipation rates of the two models. From (5.7), and noting that $\sum_i q_i \gamma_i = 0, i = 1, 2, -$, we obtain the dissipation rate of (5.7):

$$\frac{dE_v}{dt} = -2\nu_- q_- a_-^2. \tag{5.8}$$

To find an (approximate) expression for a_- in (5.8), we obtain its solution for small time from (5.7) with $a_1 \approx a_1(0), a_2 \approx a_2(0)$:

$$\frac{da_-}{dt} + \nu_- a_- = \gamma_- a_1(0) a_2(0) \cos(\mu \omega_- t/2). \tag{5.9}$$

Equation (5.9) has an analytical solution:

$$a_- = \gamma_- a_1(0) a_2(0) \left[\frac{\nu_- \cos(\mu \omega_- t/2) + \omega_-/2 \sin(\mu \omega_- t/2) - \nu_- e^{-\nu_- t}}{\nu_-^2 + \omega_-^2/4} \right]. \tag{5.10}$$

Substituting (5.10) into (5.8), taking the average, and equating the final result to (5.4), we obtain finally $v_- = v_-(\beta_-)$. The expression is complicated, but simplifies for the case of $\mu \ll 1$, after some algebra, to

$$v_- = \beta_-/4. \quad (5.11)$$

6. Numerical results

The general problem of interest contains a spectrum of incident wave components forming multiple combinations of three-wave systems of the kind we have considered. With increasing time, the amplitudes of these components evolve, forming potentially new near-resonant combinations. The extension of the analysis to include multiple/coupled (near) resonances is, in principle, possible but not straightforward. To study the long-term behaviour of multiple interacting waves and also to provide a validation of our analytical results, we utilize the highly efficient direct numerical high-order spectral (HOS) scheme (Dommermuth & Yue 1987) which has been extended to general finite depth (Liu & Yue 1998; Alam, Liu & Yue 2010). The method has been well documented and validated (see Liu & Yue 1998, for extensive convergence tests and validations) and will not be described here. For the present application, we include the damping associated with β_- in the HOS by modifying the free-surface dynamic boundary condition (Wu, Liu & Yue 2006).

For the direct numerical simulation of the present problem, we use a typical (periodic) domain length of $k_i L_x \gtrsim 16$, with $N_x = 128$ Fourier wavenumber modes, and time step $\omega_1 \Delta t, \omega_2 \Delta t \lesssim 0.1$ (in a fourth-order Runge–Kutta scheme). In all the simulations below, we use nonlinear order $M = 3$. With these parameters, all the numerical results presented are converged to $\lesssim 1\%$.

We first check the analytic prediction of the evolution of a_- given by (5.2). Figure 3(a) compares the amplitude envelop (5.2) and direct simulation results for different values of damping coefficient β_- . For $\beta_- = 0$, we see the oscillatory energy exchange between the sub-harmonic long wave and the propagating short waves due to harmonic generation. For $\beta_- > 0$, the amplitude evolutions take the form of a damped oscillation settling after long time towards a steady-state finite asymptotic value. The oscillation amplitudes become smaller with increasing β_- and eventually become over-damped beyond some critical value of $\beta_-/\omega_- \sim O(1)$. The damped oscillatory behaviour (with period close to $T_{mod} = 4\pi/(\mu\omega_-)$) is explicit in (5.2). The steady-state amplitude is given by the coefficient of (5.2) and is shown to decrease monotonically with increasing β_- . The comparisons between theoretical and direct (HOS) numerical predictions are satisfactory. The discrepancy is mainly at the (positive) peaks, where the simplifying assumption of constant a_1, a_2 in (5.2) is expected to be least valid. For the large- β_- case, for which (5.2) becomes less valid, the discrepancy is more pronounced (and more uniform in time).

The analytical behaviours of $a_1(t)$ and $a_2(t)$ obtained from quadrature of (5.7) with (5.11) are plotted in figure 3(b). The $\beta_- = 0$ case reflects the oscillatory nature of the harmonic generation energy exchange. The oscillation period (obtained from quadrature) is close to T_{mod} , consistent with the behaviour of a_- . In all $\beta_- > 0$ cases, the evolution is marked by near-monotonic (with small-amplitude modulations mainly associated with T_{mod}) decrease in amplitude of the shorter a_2 wave, (partially) compensated by the monotonic increase of amplitude a_1 of the longer primary wave. In these figures, the rate of decrease of a_2 is always greater than the rate of increase of a_1 (the total energy of the system here decreases in time according to (5.8)).

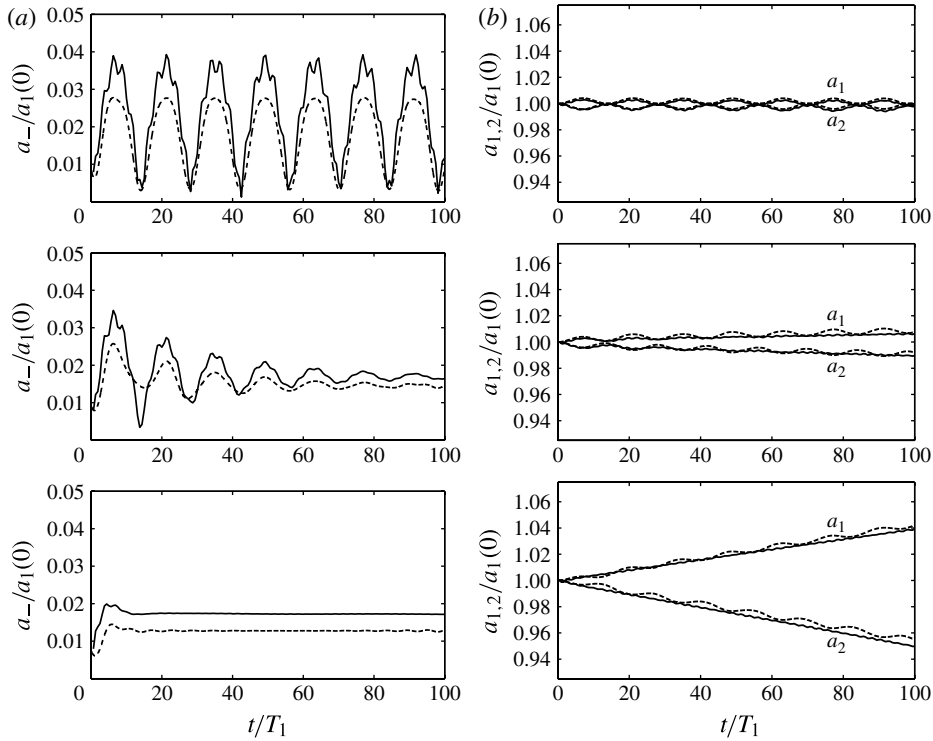


FIGURE 3. Amplitude envelope for respectively $\beta_-/\omega_- = 0, 0.09$, and 0.79 (from top to bottom). The figure validates the sub-harmonic envelope modulation by second-order theory developed here (equation (5.2), - - -) against high-order direct simulation (—). Parameters are $k_1h = 1.0$, $k_2h = 1.2$, $k_1a_1 = 0.010$, $k_2a_2 = 0.012$. Simulation parameters are $M = 3$, $N = 128$, and $T_1/\delta t = 64$.

The HOS predictions are also plotted. The comparisons with theory are remarkably satisfactory.

The results for other values of $k_{1,2}h$ show qualitatively similar features. Figure 4 compares the evolutions of primary wave amplitudes obtained with different combinations of k_1h and k_2h (with fixed k_-h and β_-). For all cases, the analytic solution compares well with the direct simulation result. For larger k_1h and k_2h , a_2 (a_1) attenuates (grows) with time at slower rate, resulting a slightly smaller total dissipation rate of the triad system (cf. figure 1a).

The total dissipation rate of the system (via damping of the long sub-harmonic wave) is a primary interest. The dissipation rate predicted from energy considerations through the evolution (5.7) is plotted in figure 1(b), compared to that obtained from direct evaluation of the power loss (equations (5.3), (5.4)). Also plotted is the HOS predictions. Qualitatively, the predictions are similar with an extremum at almost the same value of $\beta_{-max}/\omega_- \approx 0.5$. Quantitatively, (5.7) and HOS are closer since both account for the evolution of a_1 , a_2 , while (5.4) does not. The latter is strictly valid for small initial time, which is indeed the case in figure 1(b).

Note that the present work considers the dissipation rate in time (in a space-periodic system). Its counterpart, the dissipation rate in space, can be obtained by scaling the time dissipation rate by the wave group velocity (Wu *et al.* 2006; Alam, Liu & Yue 2009a,b). For the parameter $\omega_- \sqrt{h/g} = 0.17$ in figure 1(a), as an example,

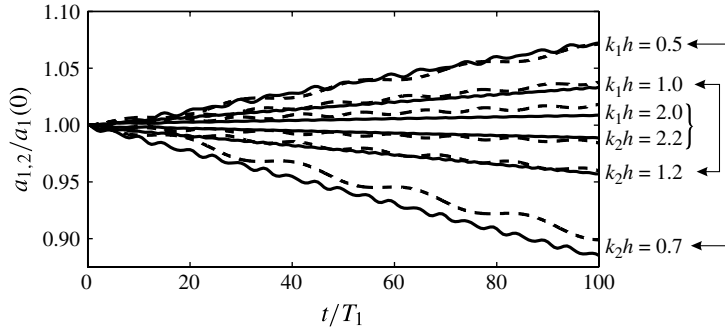


FIGURE 4. Amplitude envelope of primary short waves (a_1, a_2) for fixed $\beta_-/\omega_- = 0.06$ and $(k_2 - k_1)h = 0.2$ but different primary wavenumber combinations: $(k_1 h, k_2 h) = (0.5, 0.7)$, $(1.0, 1.2)$, and $(2.0, 2.2)$. Plotted are the analytic solution from (5.7) (---) and direct simulation (—) with initial amplitudes $a_1/h = a_2/h = 0.01$.

the space dissipation rate at respectively frequency $f = \omega/2\pi = 0.060$ Hz (0.43 Hz) and depth $h = 2$ m (4 m) in figure 3 of Elgar & Raubenheimer (2008) corresponds to dimensionless time dissipation rate $\beta/\omega \simeq 0.4$ (0.08) in figure 1(b). It is seen from figure 1(b) that the value of $\beta/\omega \simeq 0.4$ is close to the maximum dissipation rate of short waves that we predict (achieved through sub-harmonic near-resonance interactions).

We remark that figures 3(b) and 4 show the still relatively early stage of the a_1, a_2 evolution. Because of the assumptions inherent in (5.11), the theoretical results are strictly valid only up to $\epsilon\omega t = O(1)$ time. Using the HOS, we are able to perform simulations (not shown here) for much longer time (up to $\epsilon^2\omega t = O(1)$) to obtain the final asymptotic behaviours: a_1 approaching steady-state constant, and a_2 decaying to zero.

To illustrate the evolution features of multiple components of incident waves undergoing the sub-harmonic dissipation mechanism we consider, we simulate the nonlinear interactions involving multiple (near) resonances using the HOS. To isolate the sub-harmonic dissipation mechanism, we choose a relatively narrow Gaussian spectrum of short waves whose sub-harmonic long waves are damped by bottom dissipation (figure 5a). The effective wave steepness of the spectrum we use is $k_p H_s/2 = 0.06$ where k_p is the peak wavenumber and H_s the significant wave height. The spectral evolution obtained with and without the bottom dissipation is shown in figure 5(b). In the absence of bottom dissipation, the peak of the wave spectrum is only slightly decreased (due to energy transfer to sub-harmonic and superharmonic wave components). When the sub-harmonic wave dissipation effect is included, however, the spectrum is qualitatively transformed with significant amplitude attenuation and frequency downshift. For evolution times of $t/T = 500, 5000$, and 8000 (where T is the peak period), respectively, figure 5(b) shows that the total energy of the incident wave spectrum is decreased by 7%, 69% and 88%, due to the nonlinear sub-harmonic dissipation mechanism.

7. Conclusion

We consider the canonical problem of near-resonant interaction among two short propagating waves and a sub-harmonic long wave, including dissipation of the latter that may come from bottom interactions. We obtain analytic perturbation predictions

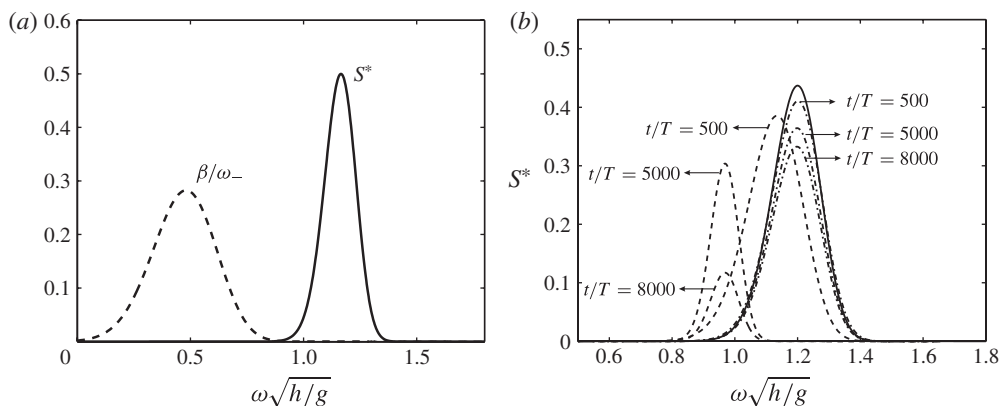


FIGURE 5. (a) Initial wave spectrum (—) and damping coefficient β normalized by $\omega_- = 0.8$ (- - -). (b) Time evolution of the wave spectrum at initial time (—) and times $t/T = 500, 5000$ and 8000 with bottom damping (- - -) and without bottom damping (- · -).

of the evolution of the amplitudes of the interacting waves: damped oscillation toward finite steady state of the sub-harmonic wave, and the overall energy loss of the short waves with decreasing/increasing amplitudes of the shorter/longer of the primary waves. An important finding is the existence of a damping coefficient value (for given primary wave frequencies and water depth) at which the energy dissipation rate of the total system is maximized. The theoretical predictions are validated against direct numerical simulations with excellent comparisons.

The present work elucidates a possible mechanism and provides quantitative predictions for significant energy transfer from short waves to long waves travelling over a dissipative bottom. Despite the canonical problem we consider involving a single triad, the results provide a physically plausible explanation of recent observations of strong short-wave attenuation as they travel over (dissipative) muddy seafloors (Sheremet & Stone 2003; Sheremet *et al.* 2005; Elgar & Raubenheimer 2008). The application of the present work to the general problem involving broadband wave spectra and multiple/coupled resonances (over bottom bathymetry), and hence possible direct comparisons to field measurements, is of practical importance and is the focus of ongoing research.

Acknowledgements

This research is supported financially by US Office of Naval Research as a part of the Multidisciplinary University Research Initiative (MURI) program under grant N00014-06-1-0718. The sponsorship is greatly acknowledged. M.R.A. acknowledges partial support from American Bureau of Shipping.

REFERENCES

- ALAM, M.-R., LIU, Y. & YUE, D. K. P. 2009a Bragg resonance of waves in a two-layer fluid propagating over bottom ripples. Part I. Perturbation analysis. *J. Fluid Mech.* **624**, 191–224.
- ALAM, M.-R., LIU, Y. & YUE, D. K. P. 2009b Bragg resonance of waves in a two-layer fluid propagating over bottom ripples. Part II. Numerical simulation. *J. Fluid Mech.* **624**, 225–253.
- ALAM, M.-R., LIU, Y. & YUE, D. K. P. 2010 Oblique sub- and super-harmonic Bragg resonance of surface waves by bottom ripples. *J. Fluid Mech.* **643**, 437–447.

- ALAM, M.-R. & MEI, C. C. 2007 Attenuation of long interfacial waves over a randomly rough seabed. *J. Fluid Mech.* **587**, 73–96.
- BRYANT, P. J. J 1973 Periodic waves in shallow water. *J. Fluid Mech.* **59** (4) 925–644.
- DALRYMPLE, R. A. & LIU, P. L.-F. 1978 Waves over soft muds: a two-layer fluid model. *J. Phys. Oceanogr.* **8** (6), 1121–1131.
- DOMMERMUTH, D. G. & YUE, D. K. P. 1987 A high-order spectral method for the study of nonlinear gravity waves. *J. Fluid Mech.* **184**, 267–288.
- ELGAR, S. & RAUBENHEIMER, B. 2008 Wave dissipation by muddy seafloors. *Geophys. Res. Lett.* **35** (7), 1–5.
- GODA, Y. 1967 Traveling secondary waves in channels. *Report to Port and Harbor Research Institute, Ministry of Transport, Japan.*
- HASSELMANN, K. 1962 On the nonlinear energy transfer in a gravity wave spectrum, part 1: general theory. *J. Fluid Mech.* **12**, 481–501.
- KAIHATU, J., SHEREMET, A. & HOLLAND, T. 2007 A model for the propagation of nonlinear surface waves over viscous muds. *Coast. Engng* **54**, 752–764.
- KIRBY, J. T. 1986 A general wave equation for waves over rippled beds. *J. Fluid Mech.* **162**, 171–186.
- LIU, Y. & YUE, D. K.-P. P. 1998 On generalized Bragg scattering of surface waves by bottom ripples. *J. Fluid Mech.* **356**, 297–326.
- MACPHERSON, H. 1980 The attenuation of water waves over a non-rigid bed. *J. Fluid Mech.* **97** (04), 721.
- MEI, C. C. 1985 Resonant reflection of surface water waves by periodic sandbars. *J. Fluid Mech.* **152**, 315–335.
- MEI, C. C., KROTOV, M., HUANG, Z. & HUHE, A. 2010 Short and long waves over a muddy seabed. *J. Fluid Mech.* **643**, 33–58.
- MEI, C. C. & UNLUATA, U. 1971 Harmonic generation in shallow water waves. In *Waves on Beaches and Resulting Sediment Transport: Proc. Advanced Seminar, Mathematics Research Center, the University of Wisconsin, and the Coastal Engineering Research Center, US Army, at Madison, October 11–13, 1971*, p. 181. Academic.
- MYRHAUG, D. 1992 Bottom Friction beneath Random Waves. *Coast. Engng* **24**, 259–273.
- NG, C.-O. & ZHANG, X. 2007 Mass transport in water waves over a thin layer of soft viscoelastic mud. *J. Fluid Mech.* **573**, 105–130.
- SHEREMET, A., MEHTA, A., LIU, B. & STONE, G. 2005 Wave sediment interaction on a muddy inner shelf during Hurricane Claudette. *Estuar. Coast. Shelf Sci.* **63** (1–2), 225–233.
- SHEREMET, A. & STONE, G. W. W. 2003 Observations of nearshore wave dissipation over muddy sea beds. *J. Geophys. Res.* **108** (C11), 1–11.
- TORRES-FREYERMUTH, A. & HSU, T.-J. 2010 On the dynamics of wave-mud interaction: a numerical study. *J. Geophys. Res.* **115** (C7), 1–18.
- WU, G., LIU, Y. & YUE, D. K. P. 2006 A note on stabilizing the Benjamin Feir instability. *J. Fluid Mech.* **556**, 45–54.
- YOUNG, I. 1998 Observations of triad coupling of finite depth wind waves. *Coast. Engng* **33** (2–3), 137–154.